SUPPORTING THEORY

Conventional MT Models

The reversible exchange process in a two-pool model can be depicted by the Bloch equations, modified with the coupling terms, which consist of a free bulk water proton pool (*w*) and a semi-solid macromolecular proton pool (*m*) (1, 2). Based on this, a CEST experiment typically involves the selective RF irradiation (ω_1) of the longitudinal magnetization associated with the semi-solid macromolecular protons and the observation of the steady-state longitudinal magnetization of the free bulk water protons, M_z^w, which has the equilibrium magnetization, M_0^w:

$$\frac{M_z^w}{M_0^w} = \frac{\frac{1}{T_{1m}}\left(RM_0^m T_{1w}\right) + R_{rfm} + \frac{1}{T_{1m}} + R}{\left(RM_0^m T_{1w}\right)\left(R_{rfm} + \frac{1}{T_{1m}}\right) + \left[1 + \left(\frac{\omega_1}{2\pi\Delta_w}\right)^2 \left(\frac{T_{1w}}{T_{2w}}\right)\right]\left(R_{rfm} + \frac{1}{T_{1m}} + R\right)} \quad [S1]$$

where T_{1w} and T_{2w} are the longitudinal and transverse relaxation times of the free water proton pool, respectively; T_{1m} and T_{2m} are the longitudinal and transverse relaxation times of the semi-solid macromolecular proton pool, respectively; and M_0^m is the fully-relaxed equilibrium magnetization value associated with the semi-solid macromolecular pool; R is the rate constant describing the magnetization exchange between the two proton pools (RM_0^m for the exchange from the water pool to macromolecule pool and RM_0^w for the reverse direction); and the RF absorption rate, R_{rfm}, is the loss rate of the longitudinal magnetization by the semi-solid pool due to the off-resonance RF irradiation of amplitude ω_1 and frequency offset Δ_w.

In the semi-solid MT model description for biological tissues, the RF absorption rate is dependent on the absorption lineshape, $g_m(2\pi\Delta_m)$, and a super-Lorentzian lineshape for the semi-solid macromolecular protons has been shown to be suitable for fitting the data acquired from a wide frequency offset (3, 4):

$$R_{rfm} = \omega_1^2 \pi g_m(2\pi\Delta_m) \quad [S2]$$

$$g_m\left(2\pi\Delta\right) = \int_0^{\pi/2} d\theta \sin\theta \sqrt{\frac{2}{\pi}} \frac{T_{2m}}{\left(3cos^2\theta - 1\right)} e^{-2\left(\frac{2\pi\Delta_m T_{2m}}{3cos^2\theta - 1}\right)^2} \quad [S3]$$

$$\Delta_m = \Delta_w + \Delta_{mw} \quad [S4]$$

where Δ_m is the frequency offset for the semi-solid macromolecular protons, and Δ_{mw} is the frequency difference between the semi-solid macromolecular protons and the free water protons.

In the sEMR[1] and sEMR[2] models ($\Delta_{mw}= 0$), the symmetric MT signal expression, as described by Eq. [S1], can be uniquely determined in terms of five combined model parameters, R, T_{1m}, T_{2m}, $RM_0^m T_{1w}$, and T_{1w}/T_{2w} (3, 4). The parameter T_{2m} is incorporated into the absorption rate, R_{rfm}, as described in Eq. [S2]. After these five model parameters are obtained by fitting the observed wide-offset MT data, the EMR spectra (Z_{EMR}) can be calculated with the corresponding ω_1 and Δ_m. For the aEMR[2] model, the MT asymmetry can be described by assuming an average frequency offset, Δ_{mw}, as shown in Eq. [S4]. The asymmetric MT signal expression can be determined in terms of six combined model parameters, R, T_{1m}, T_{2m}, $RM_0^m T_{1w}$, T_{1w}/T_{2w}, and Δ_{mw} (5).

APT-Weighted Imaging Signal and Contrast

For APT imaging, under the zero-order approximation (6):

$$\begin{aligned} MTR_{asym}(3.5ppm) &= \mathrm{MTR}(+3.5ppm, \text{label}) - \mathrm{MTR}(\text{-}3.5ppm, \text{reference}) \\ &= APTR + MTR'_{asym}(3.5ppm) \\ &\approx APTR - [NOER^{mobile}(-3.5ppm) + NOER^{less\ mobile}(-3.5ppm)] \end{aligned} \quad [S5]$$

where MTR'_{asym} is dominated by the upfield intramolecular and intermolecular NOE effects of various polypeptides, lipids, and metabolites in tissue (mobile and relatively less mobile, described by $NOER^{mobile}$ and $NOER^{less\ mobile}$, respectively). The $NOER^{less\ mobile}$ has often equivalently been thought to be the inherent MTR_{asym} of the semi-solid conventional MT effect (5-8). For aEMR[2], we define that $\delta = Z_{EMR}(3.5ppm) - Z_{EMR}(\text{-}3.5ppm) = NOER^{less\ mobile}$. The $MTR_{asym}(3.5ppm)$ images calculated by Eq. [S5] are usually called APT-weighted images (9).

Further, the APT-weighted image contrast between glioma and contralateral brain tissue can be described by:

$$\begin{aligned} \Delta MTR_{asym}(3.5ppm) &= [MTR_{asym}(3.5ppm)]_{glioma} - [MTR_{asym}(3.5ppm)]_{normal} \\ &= [APTR_{glioma} - APTR_{normal}] \\ &\quad + [NOER^{mobile}_{normal}(-3.5ppm) - NOER^{mobile}_{glioma}(-3.5ppm)] \\ &\quad + [NOER^{less\ mobile}_{normal}(-3.5ppm) - NOER^{less\ mobile}_{glioma}(-3.5ppm)] \end{aligned} \quad [S6]$$

Based on Eq. [S5], the APT-weighted MRI signal intensity quantified by $MTR_{asym}(3.5ppm)$ is reduced by the NOE effect. However, for APT-weighted MRI applications to neuro-oncology, it has been shown that the NOE effect is larger in normal brain tissue than in tumor (an image contrast opposite to that of the APT effect), and thus, increased APT-weighted image contrast between the tumor and the normal brain tissue, based on an MTR asymmetry analysis (10).

MT Model under a Non-Steady-State (NS) Condition

A conventional MT imaging experiment involves the selective RF saturation (ω_1) of the longitudinal magnetization associated with the semi-solid macromolecular protons M_z^m and the observation of the longitudinal magnetization of the free bulk water protons, M_z^w, which has the equilibrium magnetization, M_0^w:

$$dM_x^w / dt = -(1/T_{2w})M_x^w - (\omega_w - \omega)M_y^w \quad [S7]$$

$$dM_x^m / dt = -(1/T_{2m})M_x^m - (\omega_m - \omega)M_y^m \quad [S8]$$

$$dM_y^w / dt = (\omega_w - \omega)M_x^w - (1/T_{2w})M_y^w - \omega_1 M_z^w \quad [S9]$$

$$dM_y^m / dt = (\omega_m - \omega)M_x^m - (1/T_{2m})M_y^m - \omega_1 M_z^m \quad [S10]$$

$$dM_z^w / dt = \omega_1 M_y^w - (1/T_{1w})M_z^w - k_{wm}M_z^w + k_{mw}M_z^m + M_0^w / T_{1w} \quad [S11]$$

$$dM_z^m / dt = \omega_1 M_y^m - (1/T_{1m})M_z^m - k_{mw}M_z^m + k_{wm}M_z^w + M_0^m / T_{1m} \quad [S12]$$

where $M_{x,y}^{w,m}$ are the X and Y components of the magnetizations; and k_{ws} and k_{sw} are the exchange rates of protons from the free bulk water pool to the semi-solid macromolecular proton pool, and vice versa.

It is assumed that the transverse magnetizations of the two pools reach a steady state (SS) at the end of the off-resonance RF irradiation (several hundreds of milliseconds) because both T_{2w} and T_{2m} are short enough for $M_{x,y}^{w,m}$ to reach zero. Under the SS condition of the transverse magnetizations ($dM_x^w/dt = dM_y^w/dt = dM_x^m/dt = dM_y^m/dt = 0$), Eqs. [S7]-[S10] can be rewritten as:

$$M_y^{(w,m)} = -\frac{R_{rf(w,m)}}{\omega_1} M_z^{(w,m)} \quad [S13]$$

where the RF absorption rate, $R_{rf(w,m)}$, is the loss rate of the longitudinal magnetization by the free water pool or by the semi-solid pool due to the off-resonance RF irradiation of amplitude ω_1 and frequency offset, ω_w or ω_m. The RF absorption rate is defined as:

$$R_{rf(w,m)} = \frac{\omega_1^2 T_{2(w,m)}}{1+\left[T_{2(w,m)}\left(\omega_{(w,m)}-\omega\right)\right]^2} \quad [S14]$$

The differential equations for the longitudinal magnetization of the free water pool from Eqs. [S11] and [S12] can have an analytical solution as follows:

$$M_z^w(\mathrm{t}) = A_1 e^{\lambda_1 t} + A_2 e^{\lambda_2 t} + M_{ss}^w \quad [S15]$$

$$\lambda_{(1,2)} = -\frac{(1/T_{1w}+1/T_{1m})+(k_{wm}+k_{mw})+(R_{rfw}+R_{rfm})}{2} \pm \frac{\sqrt{\left[(1/T_{1m}-1/T_{1w})+(k_{mw}-k_{wm})+(R_{rfm}-R_{rfw})\right]^2+4k_{mw}k_{wm}}}{2} \quad [S16]$$

A_1 and A_2 are constants determined experimentally and $\lambda_{(1,2)}$ represents the longitudinal relaxation rates of the free water pool under the saturation of the semi-solid macromolecular proton pool. If λ_2/λ_1 is high enough and A_2/A_1 approaches zero, Eq. [S15] can be simplified to be (11, 12):

$$M_z^w(\mathrm{t}) = (\mathrm{M}_0^w - \mathrm{M}_{ss}^w)e^{\lambda_1 t} + M_{ss}^w \quad [S17]$$

The determination of the six parameters, T_{1m}, T_{2m}, T_{1w}, T_{2w}, k_{wm}, and k_{mw}, is necessary to describe the MT signal under the NS condition. T_{1m} is set as a constant value of 1.4 s because it could not be well determined from fitting. In addition, the independent measurement of T_{2w}^{obs} from a multiple-echo MRI experiment can be considered as T_{2w} due to the negligible effect of the semi-solid macromolecular proton pool (TE $\gg T_{2m}$).

1. Henkelman RM, Huang X, Xiang Q-S, Stanisz GJ, Swanson SD, Bronskill MJ. Quantitative interpretation of magnetization transfer. Magn Reson Med 1993;29:759-766.
2. Stanisz GJ, Kecojevic A, Bronskill MJ, Henkelman RM. Characterizing white matter with magnetization transfer and T(2). Magn Reson Med 1999;42:1128-1136.
3. Morrison C, Henkelman RM. A model for magnetization transfer in tissues. Magn Reson Med 1995;33:475-482.

4. Sled JG, Pike GB. Quantitative imaging of magnetization transfer exchange and relaxation properties in vivo using MRI. Magn Reson Med 2001;46:923-931.
5. Hua J, Jones CK, Blakeley J, Smith SA, van Zijl PCM, Zhou J. Quantitative description of the asymmetry in magnetization transfer effects around the water resonance in the human brain. Magn Reson Med 2007;58:786-793.
6. Zhou J, Payen J, Wilson DA, Traystman RJ, van Zijl PCM. Using the amide proton signals of intracellular proteins and peptides to detect pH effects in MRI. Nature Med 2003;9:1085-1090.
7. Pekar J, Jezzard P, Roberts DA, Leigh JS, Frank JA, McLaughlin AC. Perfusion imaging with compensation for asymmetric magnetization transfer effects. Magn Reson Med 1996;35:70-79.
8. Swanson SD, Pang Y. MT is symmetric but shifted with respect to water. In Proc 11th Annual Meeting ISMRM, Toronto, 2003. p. 660.
9. Zhou J, Blakeley JO, Hua J, Kim M, Laterra J, Pomper MG, van Zijl PCM. Practical data acquisition method for human brain tumor amide proton transfer (APT) imaging. Magn Reson Med 2008;60:842-849.
10. Heo H-Y, Zhang Y, Lee D-H, Hong X, Zhou J. Quantitative assessment of amide proton transfer (APT) and nuclear Overhauser enhancement (NOE) imaging with extrapolated semi-solid magnetization transfer reference (EMR) signals: Application to a rat glioma model at 4.7 T. Magn Reson Med 2014:DOI 10.1002/mrm.25581.
11. Quesson B, Thiaudiere E, Delalande C, Chateil JF, Moonen CT, Canioni P. Magnetization transfer imaging of rat brain under non-steady-state conditions. Contrast prediction using a binary spin-bath model and a super-lorentzian lineshape. J Magn Reson 1998;130:321-328.
12. Zhou J, Wilson DA, Sun PZ, Klaus JA, van Zijl PCM. Quantitative description of proton exchange processes between water and endogenous and exogenous agents for WEX, CEST, and APT experiments. Magn Reson Med 2004;51:945-952.

Supporting Table S1

Fitted two-pool MT model parameters for the CNAWM (C), the edema (E), and the glioma (G) (mean ± standard deviation)

EMR model	*ROI*	$R(s^{-1})$	$RM_0^m T_{1w}$	T_{1w}/T_{2w}	$T_{2m}(\mu s)$	$\Delta mw\ (ppm)$	χ^2
aEMR[2]	*CNAWM*	21.1 ± 0.5	1.46 ± 0.11	20.1 ± 0.7	23.5 ± 0.4	1.55 ± 0.13	8.8×10^{-5}
	Edema	43.9 ± 1.7	1.62 ± 0.23	14.8 ± 0.1	16.6 ± 1.2	1.26 ± 0.31	1.2×10^{-5}
	Glioma	49.9 ± 0.6	1.01 ± 0.18	12.2 ± 0.7	29.7 ± 1.0	0.51 ± 0.39	4.7×10^{-5}
	Post-hoc	C < E, G	C, E > G	C > E > G	C, G > E	C > E > G	
sEMR[2]	*CNAWM*	23.4 ± 1.9	1.56 ± 0.10	19.9 ± 1.1	22.4 ± 1.7	·	4.6×10^{-3}
	Edema	39.6 ± 1.2	1.47 ± 0.22	15.1 ± 0.7	16.3 ± 2.0	·	1.3×10^{-3}
	Glioma	46.8 ± 0.6	0.96 ± 0.13	12.2 ± 0.7	29.7 ± 0.5	·	2.2×10^{-3}
	Post-hoc	C < E, G	C, E > G	C > E > G	C, G > E		
sEMR[1]	*CNAWM*	15.0 ± 0.4	1.15 ± 0.12	23.3 ± 0.5	21.9 ± 0.7	·	4.4×10^{-5}
	Edema	23.5 ± 0.8	0.98 ± 0.23	18.0 ± 0.8	12.7 ± 0.6	·	2.5×10^{-5}
	Glioma	28.3 ± 0.8	0.67 ± 0.28	14.5 ± 0.9	23.9 ± 0.3	·	9.1×10^{-5}
	Post-hoc	C < E, G	C, E > G	C > E, G	C, G > E		

The post-hoc test was performed for $p < 0.05$: <, significantly smaller; >, significantly larger; not indicated, no significant.

Supporting Table S2

Fitted two-pool MT model parameters under steady-state (SS) and non-steady-state (NS) conditions for the CNAWM (mean ± standard deviation)

EMR model	*Saturation condition*	$R(s^{-1})$	$RM_0^m T_{1w}$	T_{1w}/T_{2w}	$T_{2m}(\mu s)$	$\Delta mw\ (ppm)$	χ^2
aEMR[2]	*SS*	21.1 ± 0.5	1.46 ± 0.11	20.1 ± 0.7	23.5 ± 0.4	1.55 ± 0.13	8.8×10^{-5}
	NS	29.5 ± 1.2	1.87 ± 0.10	16.2 ± 0.4	22.3 ± 0.5	1.42 ± 0.27	3.9×10^{-5}
sEMR[2]	*SS*	23.4 ± 1.9	1.56 ± 0.10	19.9 ± 1.1	22.4 ± 1.7	·	4.6×10^{-3}
	NS	24.9 ± 3.1	1.75 ± 0.11	18.4 ± 0.3	20.2 ± 1.5	·	5.3×10^{-4}
sEMR[1]	*SS*	15.0 ± 0.4	1.15 ± 0.12	23.3 ± 0.5	21.9 ± 0.7	·	4.4×10^{-5}
	NS	14.1 ± 1.1	1.32 ± 0.15	23.4 ± 1.3	25.3 ± 1.9	·	6.2×10^{-5}

Under the NS, T_{2w} was estimated from a dual-echo MRI experiment (TE_1/TE_2 = 10/80 ms) for the calculation of λ value in Eq. [S16].

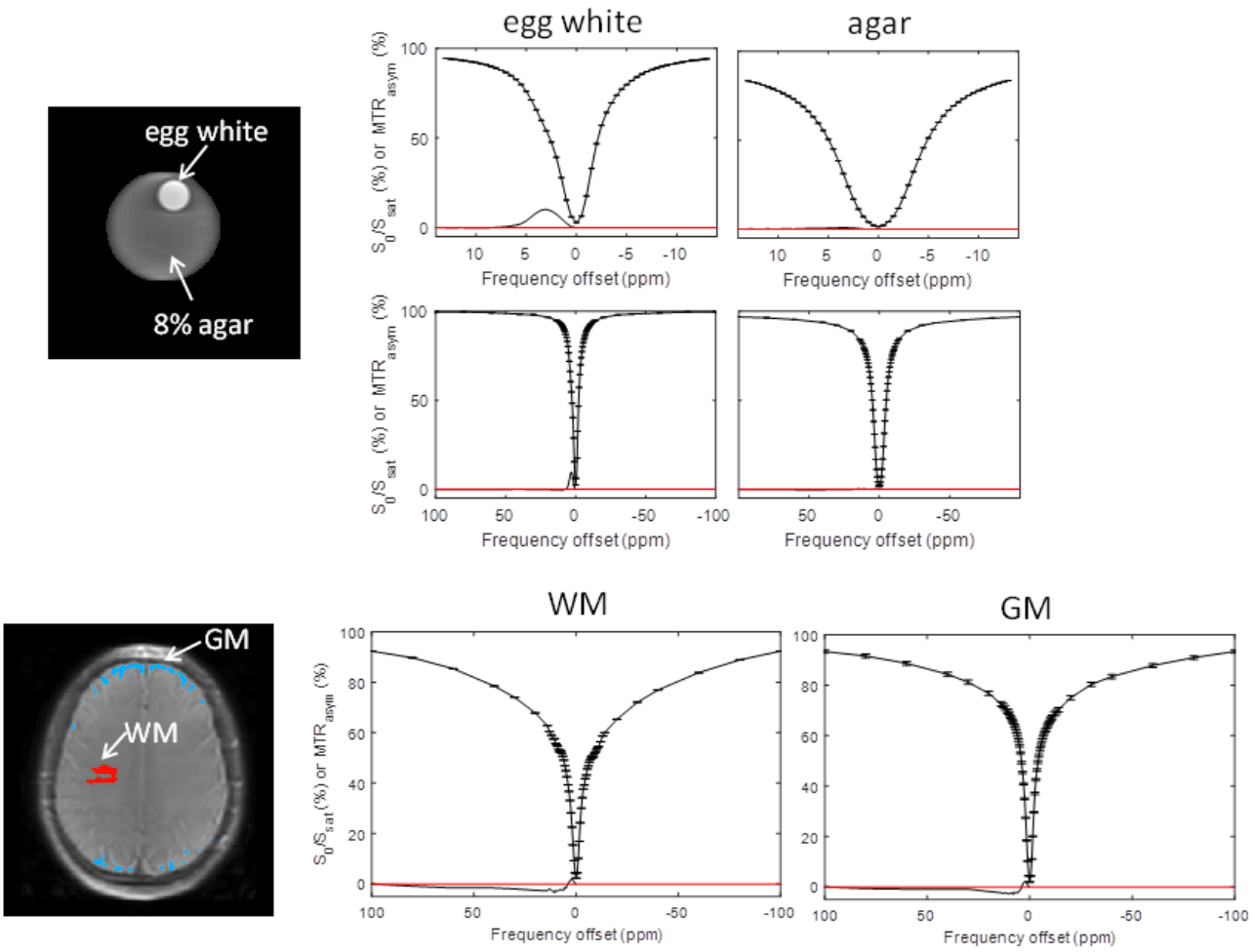

Supporting Fig. S1. CEST experimental experiments on a phantom with the egg white solution and semi-solid agar, and a healthy human subject. Unlike the in vivo case, the pure semi-solid MT (such as agar) was almost symmetric around the water signal (with -0.0003% asymmetry at 100 ppm, -0.2% asymmetry from 60 to 40 ppm). Therefore, when we say a semisolid pool with 10-μs T_2 and a shifted center frequency (e.g., -1.55 ppm), we have actually automatically included the relatively less mobile protons that cause the apparent Z-spectrum asymmetry.

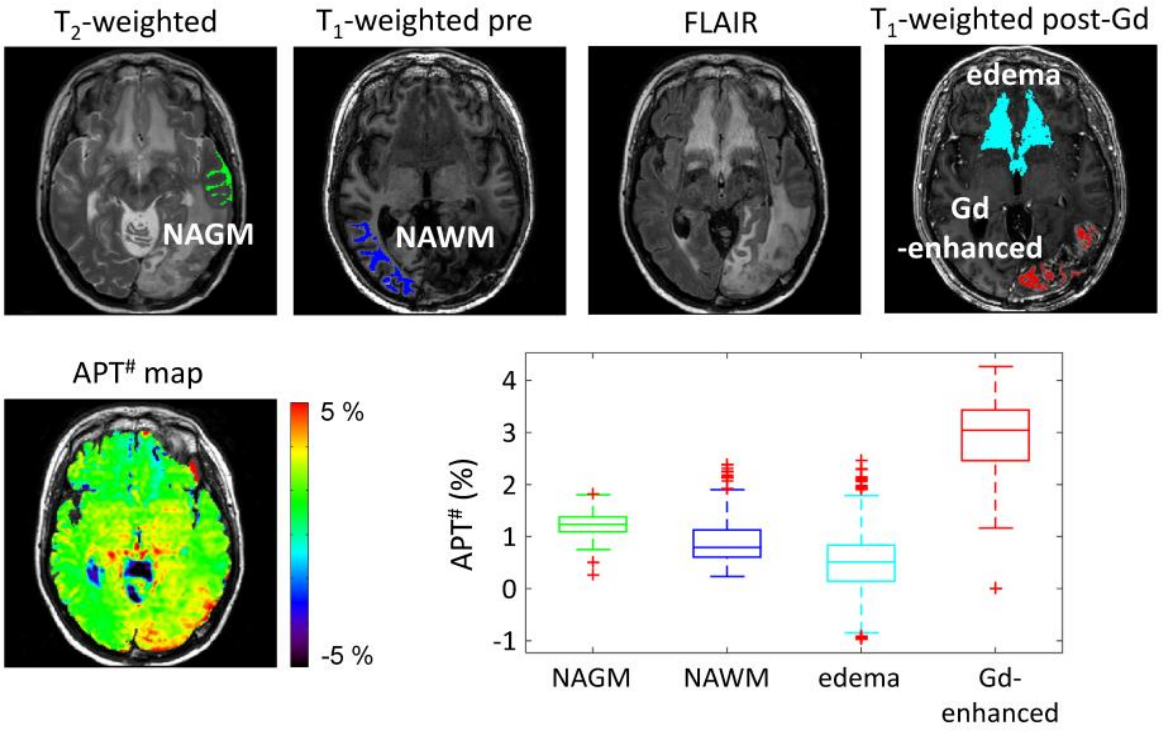

Supporting Fig. S2. Comparison of the APT$^{\#}$ signals in normal-appearing gray matter (NAGM), normal-appearing white matter (NAWM), peritumoral edema (hyperintensity in FLAIR), and Gd-enhanced tumor area. The fact that the APT signal in the Gd-enhanced tumor region was significantly higher than in the normal tissue and in the edema region showed that water T_1 is not a dominating contributor to APT signals. This is further supported by the fact (Ref. S9) that high-grade gliomas have significantly higher (hyperintense) APTw signals than low-grade gliomas (isointense), although these tumors may have similar T_1.